Spiking computation and stochastic amplification in a neuron-like semiconductor microstructure

A.S. Samardak[1,2 *], A. Nogaret[1], N.B. Janson[3], A. Balanov[4], I. Farrer[5], D.A. Ritchie[5]

[1]*Department of Physics, University of Bath, Bath, UK*
[2]*Laboratory of thin film technologies, FENU, Vladivostok, 690950, Russia*
[3]*School of Mathematics, University of Loughborough, Loughborough, UK*
[4]*Department of Physics, University of Loughborough, Loughborough, UK*
[5]*Cavendish Laboratory, University of Cambridge, Cambridge, UK*

Abstract

We have demonstrated the proof of principle of a semiconductor neuron which has dendrites, axon and a soma and computes information encoded in electrical pulses in the same way as biological neurons. Electrical impulses applied to dendrites diffuse along microwires to the soma. The soma is the active part of the neuron which regenerates input pulses of above a voltage threshold and transmits them into the axon. If two pulses diffusing along separate dendrites arrive simultaneously at the soma, these pulses interfere constructively producing a larger pulse which triggers the firing of the neuron. The neuron functions as a coincidence detector. If by contrast, sub-threshold pulses arrive with different timings, they can never combine into a larger pulse causing the neuron to remain silent. Our concept of neuron is a major step forward because its spatial structure controls the timing of pulses which arrive at the soma. Dendrites and axon act as transmission delay lines which modify the information coded in the timing of pulses. We have finally shown that noise enhances the detection sensitivity of the neuron by helping the transmission of weak periodic signals. A maximum enhancement of signal transmission was observed at an optimum noise level known as stochastic resonance. Coherence resonance and stochastic synchronization were also observed for the first time together in the same structure. The experimental results are in excellent agreement with simulations of the FitzHugh-Nagumo model. Our neuron is therefore extremely well suited to providing feedback on the various mathematical approximations of neurons.

*e-mail: asamardak@gmail.com

PACS numbers: 85.35._p, 05.45.-a, 87.85._d

I. INTRODUCTION

The effect of noise on non-linear systems is often to stabilize a regular pulsing state. A noise tuned at optimum intensity known as stochastic resonance (SR) has the power of amplifying a weak periodic signal[1-4]. SR occurs in physical systems[5-7], chemical processes[8-10], biology[11-15] and technological devices[16,17] which have in common to be bistable or to have an amplification threshold. Noise alone is able to activate coherent pulsing when the threshold is low. This coherence resonance (CR) marks the transition between spiking propelled by noise at low noise intensity and noise induced smearing described by Kramers formula[18-21]. Noise is also known to induce coordinated firing in spiral patterns in arrays of FitzHugh-Nagumo (FN) neurons[22]. The equivalent self-organization of filamentary patterns was observed in large area quantum tunnelling devices whose negative differential resistance realizes the bifurcation diagram of the FN model[23]. Advances in microfabrication now allow taking these ideas a step further in solid state 'neurons' to simulate the spatio-temporal dynamics of electric pulses[24-27].

Here we report SR and CR in a semiconductor device which mimics key functions of real neurons. The neuron uses micro-wires to channel electrical impulses to and from a central core where sum and threshold amplification takes place. The neuron empirically realizes the bifurcation diagram of the FN model and incorporates spatial elements of pulse propagation. Our experiment probes a wide range of excitations relative to the amplification threshold, the SR and CR noise levels. We show that coherence resonance appears as a noise threshold between two synchronization regimes. Below the threshold, the 'neuron' either synchronizes with the drive signal or remains silent. Above the threshold, the neuron synchronizes to its internal frequency augmented by noise. Detuning the drive frequency from the internal frequency of the neuron rapidly destroys synchronization. The data are

quantitatively explained by FN simulations provided a noisy recovery variable is considered. The present structure provides valuable experimental feedback on neuron models.

II. EXPERIMENT

Artificial 'neurons' were synthesized from GaAs/AlAs layers grown by molecular beam epitaxy according to the following sequence: *n*-type: 5 x 10^{17}cm^{-3} (80nm) / *p*-type: 5 x 10^{17}cm^{-3} (60nm) / AlAs /n^+-type: 6 x 10^{18}cm^{-3} (40nm) / p^+-type: 4 x 10^{19}cm^{-3} (500nm) / GaAs buffer. Through a combination of selective etching and lithography described elsewhere[24,25], we obtain the free standing structure which scheme shown in Fig.1a. *pn* wires form a web of micro-transmission lines which meet at the active centre of the structure or 'soma'. Depolarization waves formed across the depletion region diffuse in the plane in much the same way as action potentials do along nerve fibres because both transmission lines obey the same diffusion equation. The diffusion equation integrates in real time the delayed inputs which arrive at the 'soma'. The 'soma' lastly regenerates the combined pulses which are larger than a certain voltage threshold. This is done through the p^+n^+ tunnel device which applies positive feedback to the *pn* transmission line. To obtain the gain curve of the quantum tunnelling amplifier, we have applied rectangular pulses of height V_D and measure output pulses V_{OUT} . The gain curve presents an amplification threshold at V_{THR}=80mV which gives the 'neuron' its excitable character.

The amplification circuit (Fig.1a) incorporates the impedance of the *pn* wire in series with resistor (R), inductor (L) and soma bias (V_{SOMA}). The tunnel element also has capacitance C=1.6nF[24]. The 'Load' curve was measured and plotted as a function of the bias across the p^+n^+ layer. Quantum tunneling amplification requires that $[gR] < 1$ where g is the negative differential conductance of the tunnel diode. Experimentally, this condition is obtained for $R < 500\ \Omega$ as otherwise the 'soma' becomes bistable. We therefore choose the most favorable situation: R=0. The low regeneration threshold (80mV)[18] is obtained by placing the operation point (I_0,V_0) near the negative differential resistance region. This is done by setting V_{SOMA}=290mV. A positive pulse in the *pn* wire can provide the extra voltage needed to move

(I_0,V_0) into the negative differential resistance region and trigger amplification. The bifurcation diagram of the 'soma' experimentally realizes the null-cline curves of the FN model. The property of excitability means that sub-threshold periodic signals can be transmitted with the help of noise. We have applied a sinusoidal signal to one 'dendrite', a digitally synthesized *white noise* to another, and measure the output waveform with a DAQ acquisition card. The threshold dependence on drive frequencies in the range 1kHz-100kHz were investigated, Fig.2. At low frequencies less than 30kHz V_{THR} is very tunable and suitable for experimental procedure. Higher drive signal oscillations do not affect on V_{THR} which average value ranges from 0.1 to 0.2V.

Experimental outcomes remained qualitatively the same when *Gaussian noise* was used which suggests that the finite bandwidth of the DAQ card (2MHz) was not a limiting factor. Fig.1b shows a typical sequence of spiking events output by the 'neuron'. Noise clearly amplifies the weak periodic input although one notices that, at arbitrary noise intensity, the output partially reproduces the input signal. This behavior is in good agreement with simulations based on the semi-empirical FN equations described in [28]. The theoretical spiking sequence corresponding to the experimental conditions is shown in Fig.1b. Note, that the noise signal that reaches the soma is much smaller than at the input due to the decay in the wires.

III. RESULTS AND DISCUSSION

We experimentally study how the artificial neuron filters out noise from the input signal, and extracts the useful signal whose amplitude is considerably smaller than the noise variance. This supposedly occurs due to the SR. Within SR, the nonlinear device transforms the input signal in such a way, that at the output the useful signal is amplified, while the noise component becomes smaller. The output power of useful signal as a function of input noise intensity has a maximum at some moderate value, which means there is an *optimal value of noise* at which the device works best. Moreover, in excitable systems the *average* spiking frequency coincides with the frequency of useful signal[29,30]. A closely related effect is stochastic synchronization, which occurs if the amplitude of useful signal at the input is comparable with, although is smaller than, the threshold: the spikes appear in-phase with the useful signal most of the time, i.e. *instantaneous* frequencies coincide[30,31].

We vary both the amplitude V_D of the useful signal, and the noise strength V_N, in a wide range. First, the response to pure noise without periodic component can be characterized by two parameters: the mean spiking frequency $f_{\exp}$, and by the inverse of coefficient of variation of interspike intervals R_T , the latter being calculated as the standard deviation of interspike intervals normalized by the mean spiking period, $R_T=(Var(T))^{1/2}/<T>$. These two quantities are shown in Figs. 3(c-d) as functions of noise strength V_N by solid lines. $f_{\exp}$ is growing monotonously with noise, and $1/R_T$ displays a clear maximum at which the spiking is closest ot periodic, which is the evidence of coherence resonance (CR)[18,32]. The average spiking frequency at the CR is approximately 28kHz.

Second, we combined noise and harmonic drive with the fixed frequency of f_D=28kHz equal to the spiking frequency at CR, whose amplitude V_D was changed between 10mV and 200mV. The standard deviation of noise V_N was varied from 5mV to 600mV. At

V_D=40mV experimental signals together with their power spectral densities are illustrated in Fig. 4 at four values of V_N.

With no or vanishing noise [panel (a)], the input signals are sub-threshold, and they decay passively through the structure. Spiking bursts appear and become more frequent as the noise increases [panel (b)]. The output is closest to being periodic at noise amplitude of 130mV [panel (c)]. Further increases in noise level restore irregular spiking patterns [panel (d)]. The power spectrum, in panels (e-h), shows that the amplified frequency is the 28kHz frequency of the input drive, and that optimum amplification occurs at V_N=130mV, thus demonstrating SR.

In order to quantify the response of the neuron to a sum of periodic and random driving, we artificially decompose the output power spectral density (spectrum) into the noise background, and the peak at the driving frequency. We calculate the total power P_{tot} of the output, the P_{noi} power of noise background, and the power P_{per} of the periodic component at the frequency of periodic forcing as the integrals of the respective spectra. The more the peak at the driving frequency stands out of the noise background, the larger the P_{per} is, the spiking is closer to being periodic, and the better the useful signal is revealed at the output of the system. In what follows we will show the square roots of the powers involved, because they are proportional to the amplitudes of the respective components and can therefore be easily compared with the amplitude of periodic driving and the standard deviation of noise. At the same time, we estmate the mean spiking frequency f_{exp} and $1/R_T$ parameters.

The three powers are given in Figs. 3(a-b) as functions of noise amplitude V_N at two amplitudes of periodic driving: at V_D = 40mV (grey symbols) when the periodic forcing is essentially subthreshold, and at V_D = 70mV (white symbols) when the amplitude of periodic forcing that reaches the soma is very close to, but is slightly less than the height of the effective threshold. Both the total power P_{tot} and P_{noi} grow monotonously with noise, and

they are close to each other at very small and at very large V_N. This is understandable: at small noise there is almost no spiking, the periodic component is very small, and most of the power belongs to noise background; but at large noise the spiking is almost unaffected by periodic driving, so the total power again mostly belongs to noise. However, at moderate V_N, P_{tot} is growing faster than P_{noi}, and the difference P_{per} between them has a maximum. The latter is a clear manifestation of SR.

The spiking frequency f_{exp} is given in Fig. 3(c) by circles: at V_D = 40 mV (grey) and at V_D = 70 mV (white). At V_D = 40mV, when noise is weak ($V_N << 30$mV), spiking is very rare and is not detectable during the observation time of the experiment, therefore no frequency values are given. At $V_N > 30$mV, f_{exp} grows monotonously with noise, reaching the frequency of periodic driving f_D at V_N = 130 mV. Generally, at small V_D, the spiking frequency behaves almost in the same manner as without driving at all (see black solid line for comparison).

In Fig. 3(d) grey circles show the $1/R_T$ at V_D = 40 mV, which has a clear maximum at around V_N = 210mV. At larger V_D = 70 mV, the situation is somewhat different. At small noise (V_N < 14mV), when there is no spiking, all three powers are small. But as soon as spiking starts at $V_N \approx 14$mV, its frequency is close to that of external driving for a large range of noise intensities (Fig. 3(c), white circles), which is a manifestation of stochastic synchronization. With this, the total power P_{tot} jumps abrupty to a larger value and remains almost constant in the same range of V_N (Fig. 3(a), white circles), while the power of noise background slowly grows (white triangles). As a result, the power of periodic component abruptly jumps to a large value, and then slowly decays (Fig. 3(b), white circles). Therefore, as long as the periodic driving stays subthreshold, SR occurs. At the same time, the coherence factor $1/R_T$ displays a clear maximum (d) which is also an evidence of SR.

At the suprathreshold values of V_D > 75mV, one can regard spiking in the neuron as the periodic oscillations induced by periodic driving and *influenced* by noise. These oscillations are *no longer noise-induced*, and noise can only smear them. Therefore, one cannot expect any nontrivial stochastic phenomena like SR here, and P_{per} or $1/R_T$ can only monotonically decrease with noise. The transition from noise-induced to noise-smeared oscillations is illustrated in Fig. 5 (a) where P_{per} is shown as a function of two parameters: V_D and V_N. At the same time, the stochastic synchronization is illustrated by (b) where f_{exp} is shown for the same parameters. A triangular plateau is the region where either the stochastic spiking is locked by external subthreshold periodic driving (V_D < 75mV), or the perio dic spiking is affected by noise (V_D > 75mV). The experimental results reported abov e can be modeled by deriving an approximate model of the artificial neuron from the first principles. We assume that the dendrites carrying the input signals (noise and per iodic driving) to the soma only attenuate them, but otherwise do not transform them. The experimental results are in excellent agreement with simulations of the FitzHugh-Nagumo model whose two equations derive from the equations of the soma circuit[28]. The parameters of the FitzHugh-Nagumo model are calculated through simple algebraic expressions directly from the nominal parameters of the semiconductor structure. Our neuron is therefore extremely well suited to providing feedback on the various mathematical approximations of neurons.

CONCLUSIONS

The paper is devoted to experimentally prove the principle of a semiconductor device mimicking the electrical activity of real neurons. The advantage of our device over VLSI neurons resides in its spatially extended structure which enables electrical pulses to propagate in and out of the soma via artificial nerve fibres. Real neurons encode information in both the frequency and the timing of electrical pulses and use nerve capillaries as transmission delay lines to control their timing. Our neuron uses semiconductor micro-wires as artificial nerve fibres. A tunnelling amplifier forms the active part of the structure, or 'soma', and whose function is to regenerate pulses above a voltage threshold. We have demonstrated the transmission of sub-threshold periodic signals in the presence of noise and show that the artificial neuron uses noise in the same constructive way as biological neurons to detect vanishingly small signals. We demonstrated stochastic resonance by computing the Fourier power of the output signal and the variance of inter-spike intervals. We studied stochastic resonance and coherence resonance as a function of the frequency and amplitude of the drive signal, the regeneration threshold and the noise level to evidence stochastic synchronization near the regeneration threshold. The versatility of the neuron has for the first time enabled the simultaneous observation of all three stochastic phenomena and their interactions.

Our results are of interest to the microelectronics industry and the general public. Like the transistor, the proposed neuron is an active analogue device which is monolithic and scalable. Whereas the transistor was designed for current amplification, the present neuron is a parallel processor which is bound to form the building block of neural computers. Pulsing neurocomputers have applications to human-computer interfaces, prothetic devices and powerful neural classifiers.

Acknowledgments

AS, AN, IF and DAR acknowledge the support of Leverhulme Trust under grant (F/0035/N) and thank Stephen Taylor for help with graphics design. NBJ acknowledges the support of EPSRC (UK).

REFERENCES

1. K. Wiesenfeld and F. Moss, Nature 373, 33 (1995).

2. K. Park and Y.-C. Lai, Europhys.Lett. 70, 432 (2005).

3. L. Gammaitoni, F. Marchesoni, and S. S., Phys. Rev. Lett. 74, 1052 (1995).

4. B. McNamara and K. Wiesenfeld, Phys. Rev. A 39, 4854 (1989).

5. B. McNamara, K. Wiesenfeld, and R. Roy, Phys. Rev. Lett. 60, 2626 (1988).

6. A. Grigorenko, P. Nikitin, A. Slavin, and P. Zhou, J.Appl.Phys. 76, 6335 (1994).

7. I. Lee, X. Liu, B. Kosko, and C. Zhou, Nano Lett. 3, 1683 (2003).

8. D. Leonard and L. Reichl, Phys.Rev.E 49, 1734 (1994).

9. M. Dykman, T. Horita, and J. Ross, J.Phys.Chem. 103, 966 (1995).

10. A. Guderian, G. Dechert, K. Zeyer, and F. Schneider, J.Phys.Chem. 100, 4437 (1996).

11. F. Moss, L. Ward, and W. Sannita, Clinical Neurophysiology 115, 267 (2004).

12. K. Kitajo, D. Nozaki, L. Ward, and Y. Yamamoto, Phys. Rev. Lett. 90, 218103 (2003).

13. T. Mori and S. Kai, Phys. Rev. Lett. 88, 218101 (2002).

14. W. Stacey and D. Durand, J. Neurophysiol. 83, 1394 (2000).

15. E. Simonotto et al., Phys. Rev. Lett. 78, 1186 (1997).

16. R. Mantegna and B. Spagnolo, Phys.Rev.E 49 (1994).

17. S. Fauve and F. Heslot, Phys. Lett. A 97, 5 (1983).

18. A. Pikovsky and J. Kurths, Phys. Rev. Lett. 78, 775 (1997).

19. C. Palenzuela, R. Toral, C. Mirasso, O. Calvo, and G. J.D., Europhys.Lett. 56, 347 (2001).

20. D. Postnov, S. Han, T. Yim, and O. Sosnovtseva, Phys.Rev.E 59 (1999).

21. G. Escalera Santos, M. Rivera, and P. Parmananda, Phys. Rev. Lett. 92, 230601 (2004).

22. P. Jung and G. Mayer-Kress, Phys. Rev. Lett. 74, 2130 (1995).

23. F.-J. Niedernostheide, M. Ardes, M. Or-Guil, and H.-G. Purwins, Phys. Rev. B 49, 7370 (1994).

24. A. Samardak et al., New.J.Phys. 10, 083010 (2008).

25. A. Samardak et al., Appl.Phys.Lett. 073502, 230601 (2007).

26. A. Nogaret, N. Lambert, S. Bending, and J. Austin, Europhys.Lett. 68, 874 (2004).

27. J. Nagumo, S. Arimoto, and S. Yoshizawa, Proc. IRE 50, 2061 (1962).

28. A. Samardak, A. Nogaret et al., Phys. Rev. Lett. 102, 226802 (2009).

29. B. Lindner, J. Garcia-Ojalvo, A. Neiman, and L. Schimansky-Geier, Physics Reports 392, 321 (2004).

30. L. Gammaitoni, P. Hanggi, P. Jung, and F. Marchesoni, Rev. Mod. Phys. 70, 223 (1998).

31. B. Shulgin, A. Neiman, and V. Anishchenko, Phys. Rev.Lett. 75, 4157 (1995).

32. H. Gang, T. Ditzinger, C. Ning, and H. Haken, Phys. Rev. Lett. 71, 807 (1993).

FIGURE CAPTIONS

FIG. 1: (a) Solid state 'neuron' excited by a sinusoidal drive (V_D) and white noise (V_N). Depolarization waves emanating from input contacts diffuse along the *pn* wire and interfere in the central region before reaching the output. The p^+n^+ tunnel layers are the pillars supporting the free standing *pn* lines. (b) Experimental and calculated sequence of spiking events corresponding to V_N=100mV, V_D=40mV and f=28kHz.

FIG. 2. The dependence of threshold voltage V_{thr} on frequency of driving signal. Insert: The magnified image of central part.

FIG. 3: Characteristics of stochastic oscillations as functions of noise strength V_N. Left: in experiment at V_D=40mV (grey) and V_D=70mV (white). Right: in simulations at V_D=0.08 (grey) and V_D=0.128 (white). Output power (square root): (a),(e) total P_{tot} (circles), of noise background P_{noi} (triangles); (b),(f) of periodic component P_{per}. Mean spiking frequency: (c) f_{exp} in experiment, (g) f_{sim} in simulation. (d),(h) Coherence $1/R_T$ of interspike intervals. In (c-d),(g-h) solid line shows functions at V_D = 0mV.

FIG. 4: Signals at the input or output of the “neuron” and their spectra. (a)-(d) Noise (black), periodic driving with *VD* = 40mV and *fD* = 28kHz (dashed grey) and response *V*out (solid grey); (e)-(h) aplitude spectra of signals in (a)-(d). Noise intensity *VN* is given on the right of each row. For clarity, the noise in (a)-(d) is shown attenuated by a factor 10.

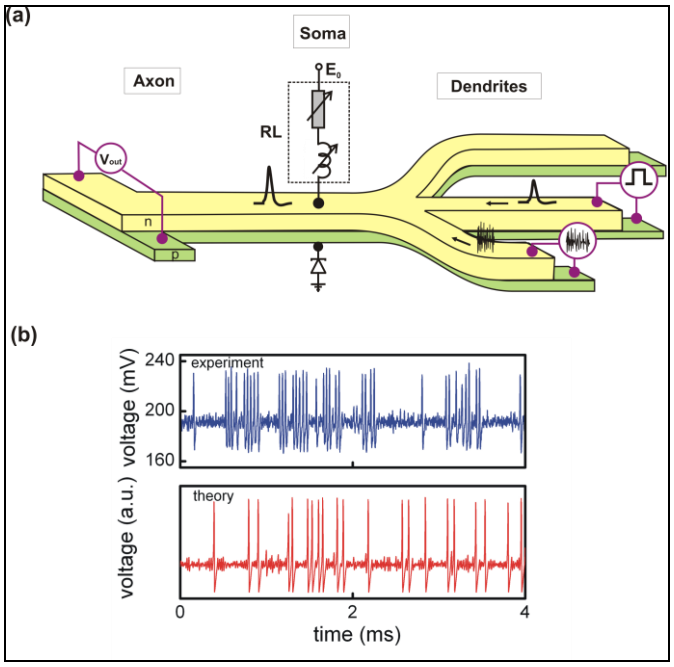
(a)
Soma
Axon
Dendrites
RL
E_0
V_{out}
n
p
(b)
240
200
160
experiment
theory
voltage (mV)
voltage (a.u.)
0
2
4
time (ms)

FIGURE 1

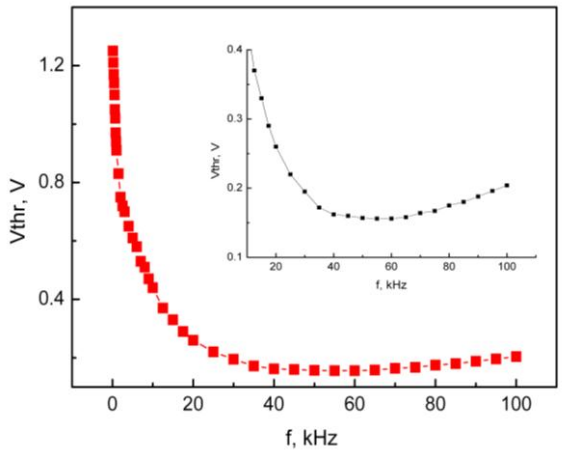
Vthr, V
1.2
0.8
0.4
0
20
40
60
80
100
f, kHz
0.4
0.3
0.2
0.1
Vthr, V
20
40
60
80
100
f, kHz

FIGURE 2

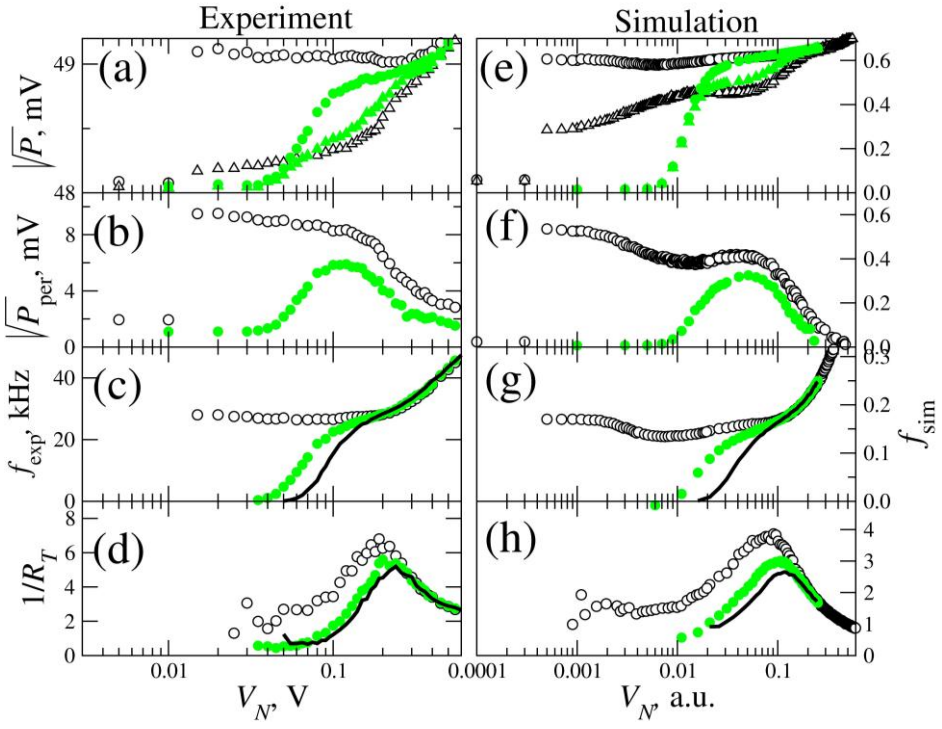
Experiment
Simulation
(a)
(b)
(c)
(d)
(e)
(f)
(g)
(h)
$\sqrt{P}$, mV
$\sqrt{P_{per}}$, mV
f_{exp}, kHz
$1/R_T$
f_{sim}
V_N, V
V_N, a.u.

FIGURE 3

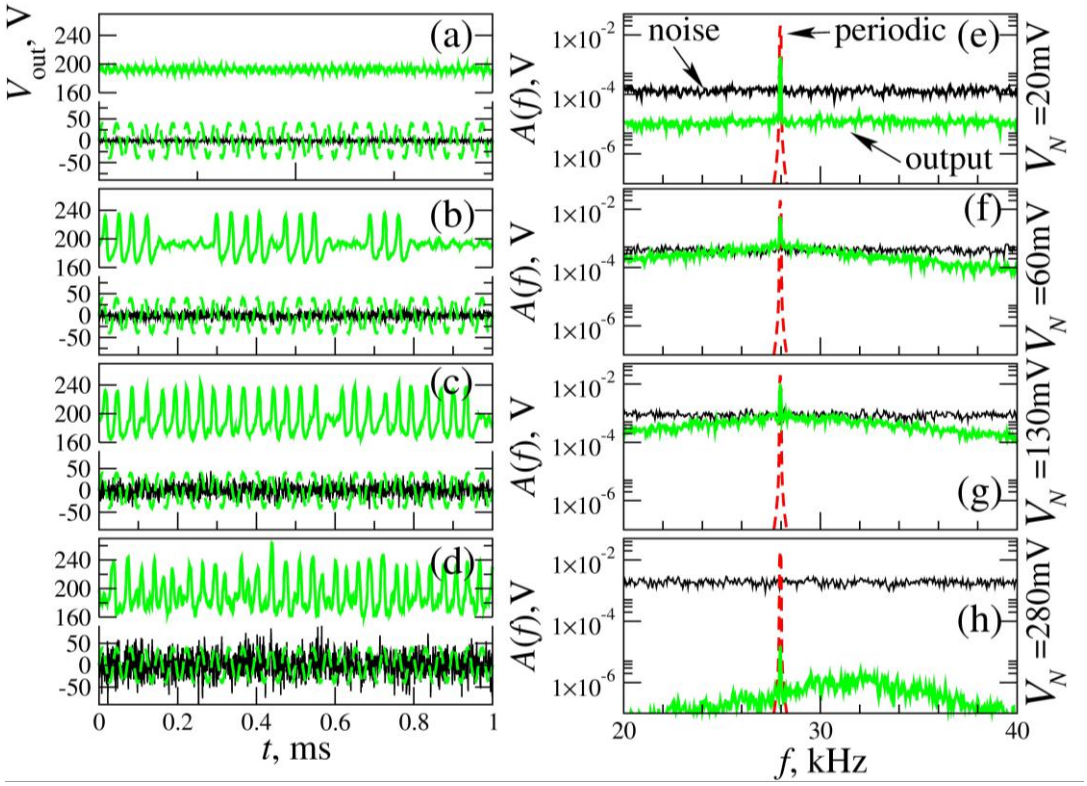
(a)
(b)
(c)
(d)
(e)
(f)
(g)
(h)
V_{out}, V
240
200
160
50
0
-50
0
0.2
0.4
0.6
0.8
1
t, ms
$A(f)$, V
1×10^{-2}
1×10^{-4}
1×10^{-6}
noise
periodic
output
V_N =20mV
V_N =60mV
V_N =130mV
V_N =280mV
20
30
40
f, kHz

FIGURE 4